THE JOURNAL OF PHYSICAL CHEMISTRY B

Article

pubs.acs.org/JPCB

Out-of-Phase Electron Spin Echo Studies of Light-Induced Charge-Transfer States in P3HT/PCBM Composite

Ekaterina A. Lukina,[†,‡] Alexander A. Popov,[†,‡] Mikhail N. Uvarov,[†] and Leonid V. Kulik*[,†,‡]

[†]Voevodsky Institute of Chemical Kinetics and Combustion of the Siberian Branch of the Russian Academy of Sciences, Institutskaya 3, Novosibirsk 630090, Russia

[‡]Novosibirsk State University, Pirogova 2, Novosibirsk 630090, Russia

Supporting Information

ABSTRACT: The light-induced charge-transfer (CT) state in the composite of the conductive polymer poly(3-hexylthiophene) (P3HT) and the fullerene derivative [6,6]-phenyl-C_{61}-butyric acid methyl ester (PCBM) has been studied by electron spin echo (ESE) spectroscopy. The out-of-phase ESE signal corresponding to the spin-correlated radical pair $P3HT^+/PCBM^-$ has been observed in this composite material. The time-domain ESE shape for different delays between the laser flash and the microwave pulse sequence has been analyzed. In order to explain the evolution of the out-of-phase ESE signal as a function of the delay between the microwave pulses, a model of the CT state is proposed. The hole is assumed to be delocalized on the P3HT chain over several thiophene subunits, while the point-dipole approximation is used to describe the interaction with the electron on PCBM. The distribution of distances between the positive and negative charges in the CT state has been evaluated.

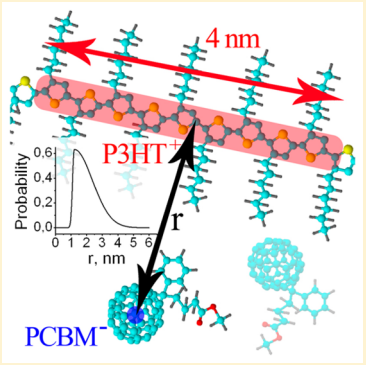

INTRODUCTION

Organic photovoltaics is an emerging alternative source of energy.[1,2] Light-induced charge separation is a key process of photoelectric conversion in organic photovoltaic cells. The most widely used active media for such devices are polymer/fullerene bulk-heterojunction blends. The power conversion efficiency of organic photovoltaic cells is determined to a large extent by the yield of photoinduced charge separation. For many polymer/fullerene blends, including the benchmark composite of the conductive polymer poly(3-hexylthiophene) (P3HT) and the fullerene derivative [6,6]-phenyl-C_{61}-butyric acid methyl ester (PCBM) (Figure S1 in the Supporting Information), this yield is close to unity.[3,4] However, the origin of such a high efficiency of charge separation is still unclear, despite numerous studies.[5−7] The main reason for this is the lack of information about the structure and dynamics of the intermediates of charge separation at the polymer−fullerene interface. These intermediates are usually called light-induced primary charge-separated states[8] or charge-transfer (CT) states,[9,10] although a number of other terms have been used as well.[11] The principal question regarding the mechanism of charge separation in polymer/fullerene (or, more generally, in donor/acceptor) composites is how the Coulomb attraction in the CT state is overcome to produce separated charges. To answer this question, knowledge of the distance between the charges in the CT state is required. Examples of the direct determination of this distance are rare.[12,13] This task is complicated by the short lifetime of the CT state at room temperature. However, the CT state can be trapped at low temperature, where the charge separation is slowed down. Under such conditions, electron paramagnetic resonance (EPR) spectroscopy becomes a suitable method to study the structure of the CT state.

Previously, time-resolved (TR) EPR spectra were obtained for the CT state in a P3HT/PCBM composite.[8−10,14,15] It has been well-established by these studies that the light-induced CT state in the P3HT/PCBM composite is a spin-correlated radical pair (SCRP) consisting of two weakly interacting radicals (polarons), $P3HT^+$ and $PCBM^-$, created in the singlet spin state upon exciton dissociation. Also, other polythiophene/fullerene[16] and oligothiophene/fullerene composites[17] have been studied by TR EPR spectroscopy. However, the interpretation of TR EPR spectra of polymer/fullerene composites is ambiguous because of the limited time resolution and complexity of the system. Pulse EPR methods based on registration of the electron spin echo (ESE) signal allow variation of many experimental parameters (intervals between microwave pulses, duration and amplitude of these pulses). Thus, they can provide additional information about the structure of this SCRP.[18] To date, only in-phase ESE has been obtained for this system, which gives some estimation of the distance between the polarons in the CT state.[19] However, these experiments do not provide detailed data on the distribution of the distances between the radicals in the pair. Such information can be obtained from the out-of-phase ESE, a powerful tool to study SCRPs.[20,21] The modulation of the out-

Special Issue: Wolfgang Lubitz Festschrift

Received: March 5, 2015
Revised: April 11, 2015
Published: April 13, 2015

DOI: 10.1021/acs.jpcb.5b02142
J. Phys. Chem. B 2015, 119, 13543−13548

of-phase ESE provides a direct measure of the strength of the magnetic interactions (dipolar and exchange interactions) between the spins composing the pair. Previously, this technique was successfully used to determine the structure of the intermediates of light-induced charge separation in bacterial photosynthetic reaction centers (RCs)[22−25] and plant photosystems.[25−29] For these systems, out-of-phase ESE gives a unique possibility to determine the interspin distance in the nanometer range with angstrom precision. The high-field out-of-phase ESE studies allow the relative orientation of photosynthetic cofactors to be determined.[30] Recently, out-of-phase ESE was used to study intramolecular light-induced charge transfer in an artificial donor−spacer−acceptor system.[31,32] To date, no out-of-phase ESE signal has been detected in polymer/fullerene bulk-heterojunction blends, and the full potential of ESE spectroscopy has not been exploited yet. Here we report the first observation of this signal in a P3HT/PCBM composite and propose an ESE-based model of the structure of the CT state.

EXPERIMENTAL SECTION

PCBM was purchased from Aldrich. Regioregular P3HT with molecular weight approximately 20−40 kDa was obtained from BASF (Sepiolid P200). Both PCBM and P3HT were used without further purification. P3HT and PCBM (1:1 weight ratio) were dissolved in chlorobenzene and mixed using an ultrasonic mixer (QSonica Microson XL2000). Several freeze−pump−thaw cycles were performed, after which the solvent was evaporated and the sample tube (5 mm o.d.) was pumped. Samples were annealed at 10^{-2} Torr and 150 °C for about 10 min, filled with ethanol, and then immediately frozen. The P3HT/PCBM composite was not affected by ethanol, since nearly the same experimental results were obtained without ethanol addition. The only difference was that fracture of the composite film under the action of laser pulses was prevented for ethanol-filled samples. A light guide was frozen into the ethanol to achieve better light irradiation. Between measurements the sample was stored in liquid nitrogen in order to avoid degradation.

All of the measurements were performed on a Bruker Elexsys E 580 X-band EPR spectrometer. An ER4118X-MD-5W1 dielectric resonator inside an Oxford ESR 900 cryostat was used. The employed microwave frequency was about 9.63 GHz. The temperature was set using an Oxford ITC 503 temperature controller and additionally monitored by an ER4131VT device. A temperature of 65 K was achieved by liquid nitrogen overpumping. The sample was irradiated by second-harmonic pulses from a Surelite-10 Nd:YAG laser with a wavelength of 532 nm, pulse duration of 10 ns, and a pulse repetition rate of 10 Hz. The incident light intensity on the sample was about 0.6 mJ. After the laser flash, a two-pulse microwave sequence was applied to form the ESE signal. The nominal durations of the nonselective microwave pulses were set to 8 and 16 ns, and their amplitudes were optimized to maximize the out-of-phase ESE intensity. It should be noted that the real duration of the pulses was shorter because of the finite rise time of the microwave field in the resonator. Therefore, the turning angle of the first nonselective pulse was smaller than $\pi/2$. This is important for producing out-of-phase ESE, since it has zero intensity if the turning angle of the first nonselective pulse exactly equals $\pi/2$.[33] In some experiments, selective $\pi/2$ and π microwave pulses with durations of 40 and 80 ns were used. In order to suppress resonator ringing and the free induction decay caused by the second microwave pulse, two-step phase cycling was applied, i.e., the measurements with positive sign and negative sign of the first pulse were subtracted. Unless otherwise specified, the time dependences of the ESE were measured at a field strength of 3448.3 G, which is approximately at the center of the echo-detected (ED) spectrum, using an integration gate of 72 ns for short pulses and 172 ns for long pulses.

RESULTS AND DISCUSSION

1. Time-Domain Shape of the ESE Signal. In our experiments, the CT state in the P3HT/PCBM composite was created by laser flashes. Since the background signal of thermalized $P3HT^+$ and $PCBM^-$ radicals complicates the ESE signal in this experiment,[18,19] we start from the analysis of the ESE shape in the time domain. The echo signal in the P3HT/PCBM composite in the time domain is not bell-shaped, in sharp contrast to the case of bacterial RCs and plant photosystems. This is caused by the narrow features of the EPR spectrum of $P3HT^+$ and $PCBM^-$ (see the continuous-wave (CW) EPR spectrum of thermalized radicals in this composite under continuous illumination,[18] shown in Figure S2 in the Supporting Information). As can be seen from Figure 1a,

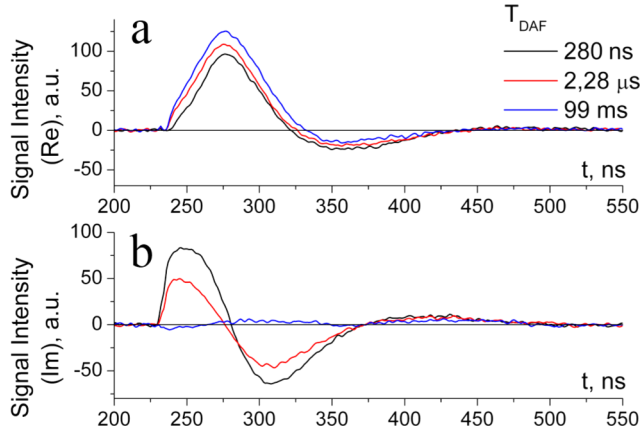

Figure 1. (a) In-phase and (b) out-of-phase echo shapes measured with T_{DAF} = 280 ns, 2.28 μs, and 99 ms (black, red, and blue lines, respectively) after the laser flash. The two-pulse microwave sequence with nonselective pulses and τ = 120 ns was used. The temperature was 65 K.

only the in-phase ESE is present for long delay times after the flash (T_{DAF} = 99 ms, limited by the shot repetition time of 100 ms). This is expected for a spin system in thermal equilibrium. T_{DAF} = 99 ms is much longer than the spin−lattice relaxation times of both $P3HT^+$ and $PCBM^-$ at 65 K, which are in the range of several tens of microseconds to several milliseconds as estimated from inversion−recovery experiments (data not shown). Thus, we conclude that for T_{DAF} = 99 ms the spins of $P3HT^+$ and $PCBM^-$ that survive recombination are relaxed to thermal equilibrium. The data for T_{DAF} = 99 ms are considered as a background. They are subtracted when necessary to obtain the flash-induced ESE signal originating from the CT state.[19]

For a smaller T_{DAF} of 2.28 μs, the out-of-phase component of the ESE appears (Figure 1b). However, it has nearly symmetric positive and negative parts, which yields zero signal intensity upon integration in the time domain. Finally, for the smallest T_{DAF} of 280 ns, the out-of-phase ESE line shape becomes

DOI: 10.1021/acs.jpcb.5b02142
J. Phys. Chem. B 2015, 119, 13543−13548

nonsymmetric and produces a positive signal upon time-domain integration. A nonzero out-of-phase ESE is a signature of a SCRP.[34]

2. Echo-Detected EPR Spectra. The in-phase components of the ED EPR spectra of the P3HT/PCBM composite measured at different T_{DAF} values are shown in Figure 2a. As

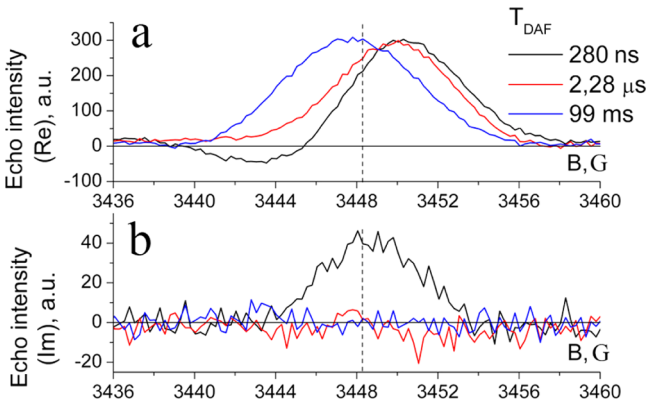

Figure 2. (a) In-phase and (b) out-of-phase echo-detected EPR spectra of P3HT/PCBM measured under pulse laser excitation. Spectra with delays of 280 ns, 2.28 μs, and 99 ms between the laser flash and the microwave pulse sequence [mw pulse (8 ns)−τ (120 ns)−mw pulse (16 ns)] are indicated by black, red, and blue lines, respectively. The dashed line indicates the field position where the echo shapes and ESE decay were measured (3448.3 G). The temperature was 65 K.

explained above, the spectrum for T_{DAF} = 99 ms corresponds to the thermalized species. No separate peaks of $P3HT^+$ and $PCBM^-$ are seen because the lines are broadened as a result of the strong magnetic field B_1 during the short nonselective microwave pulses. Such separate peaks can be obtained in an analogous experiment with weaker and correspondingly longer microwave pulses[18] (Figure S3a in the Supporting Information). The in-phase ED EPR spectra for smaller T_{DAF} values are noticeably shifted, and the spectrum for T_{DAF} = 280 ns demonstrates an emission/absorption (E/A) pattern. The flash-induced ED EPR spectrum (Figure S4 in the Supporting Information) obtained as differences of two spectra recorded at different T_{DAF} values are similar to previously published ones for T = 80 K.[18,19] In principle, nuclear ESE envelope modulation (ESEEM) can influence ED EPR spectra. However, since the amplitude of this ESEEM is negligible for $P3HT^+$ and $PCBM^-$,[18] it does not noticeably affect the ED EPR spectra in Figure 2.

The out-of-phase ED EPR spectrum for T_{DAF} = 280 ns is a single broad line (Figure 2b). Its center nearly coincides with the center of the ED EPR spectrum of the thermalized species, similar to the case of a photosynthetic SCRP.[35] Notably, the out-of-phase ESE disappears for T_{DAF} = 2.28 μs and T_{DAF} = 99 ms.

3. ESE Decay. The evolution of the out-of-phase ESE amplitude as a function of the delay between the microwave pulses, τ, was obtained by numerical integration of the time-domain echo signals measured for different delay values and is shown in Figure 3. The integration gate with a length of 120 ns was placed symmetrically with respect to the in-phase echo maximum such that almost the whole ESE signal was integrated. The behavior of the out-of-phase ESE in the P3HT/PCBM composite can be explained consistently in the

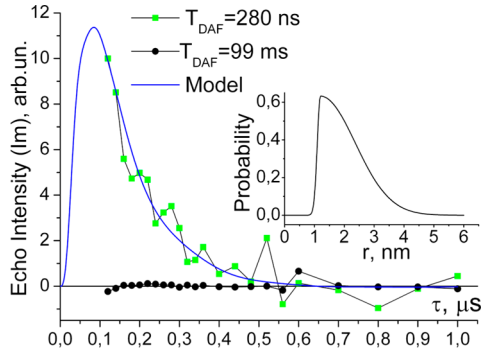

Figure 3. Out-of-phase (Im) echo decay obtained by numerical integration (gate = 120 ns) of echo shapes measured with different delays between microwave pulses. Green squares represent T_{DAF} = 280 ns; the background signal measured at T_{DAF} = 99 ms is indicated by black dots. The simulation shown by the blue line was obtained using the radical pair distance distribution shown in the inset.

framework of the SCRP model. In particular, the out-of-phase ESE disappears for the case of a selective pulse sequence $\pi/2 - \tau - \pi$ (Figure S3b in the Supporting Information), as the SCRP theory predicts.[34,33] The dependence of the out-of-phase ESE on τ is quite sharp. Apparently, it decays much faster than $\exp(-2\tau/T_2)$, where T_2 = 0.87 μs as measured for the in-phase flash-induced ESE decay of $P3HT^+$ (Figure S5 in the Supporting Information).

In order to explain the observed τ dependence of the out-of-phase ESE, we propose the following model for the CT state (Figure 4). The positive polaron is assumed to be delocalized

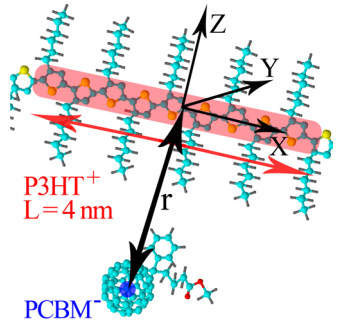

Figure 4. Model of the light-generated CT state at the P3HT−PCBM interface. The hole is assumed to be delocalized on the P3HT chain over L = 4 nm (approximately 10 thiophene monomers); the spin of the electron on PCBM is approximated as a point dipole. The principal axes of the dipolar interaction tensor are shown.

on one P3HT chain. Its spin density is approximated by a homogeneous one-dimensional distribution in a rod of length L = 4 nm. This rather crude approximation, however, reflects the delocalization of the $P3HT^+$ polaron on approximately 10 thiophene monomer subunits[36,37] and thus is more realistic than the point-dipole approximation used previously.[19] The point-dipole approximation is used for $PCBM^-$ since it is not expected to be significantly delocalized. The $PCBM^-$ point dipole is placed symmetrically at a distance r from the center of the $P3HT^+$ spin distribution. Since the point-dipole approximation no longer holds, the frequency of the dipolar oscillation of the ESE, ω_D, is determined by the components of the dipolar interaction tensor D_{ij} $(i, j = x, y, z)$:

DOI: 10.1021/acs.jpcb.5b02142
J. Phys. Chem. B 2015, 119, 13543−13548

$$D_{ij} = g_1 g_2 \mu_B{}^2 \left\langle \frac{\delta_{ij}}{R^3} - 3\frac{R_i R_j}{R^5} \right\rangle \quad (1)$$

where δ_{ij} is the Kronecker delta, R is the magnitude of the vector connecting the two electron spins, and the average is taken over R because of the spin density distribution. When the principal values of the dipolar interaction tensor D_{xx}, D_{yy}, and D_{zz} are known, the dipolar frequency can be calculated:

$$\omega_D = 2\pi\left(\frac{D_{zz}}{2}(1 - 3\cos^2\theta) + \frac{D_{yy} - D_{xx}}{2}\sin^2\theta\cos 2\phi\right) \quad (2)$$

where θ and φ are the polar and azimuthal angles, respectively, of the magnetic field B_0 in the reference frame determined by the principal axes of D_{ij} (see Figure 4). The second term in eq 2 reflects the deviation of the spin density distribution from axial symmetry. Finally, the distribution over the distance, $G(r)$, is introduced because of the intrinsic disorder of bulk-heterojunction blends. Within this model, the out-of-phase ESE intensity $M_x(\tau)$ can be calculated by the integration

$$M_x(\tau) = \int G(r)\,\mathrm{d}r \int \sin[\omega_D(\theta, \phi, r)\tau]\sin\theta\,\mathrm{d}\theta\mathrm{d}\phi \quad (3)$$

Equation 3 is valid for arbitrary shape of EPR spectrum of SCRP if it is excited uniformly by microwave pulses.

The resulting distribution over r is shown in the inset of Figure 3. We suggest a simple model function consisting of two halves of Gaussian distributions: $G(r) = \exp[-(r - r_0)^2/a^2]$ for $r < r_0$ and $G(r) = \exp[-(r - r_0)^2/b^2]$ for $r > r_0$, with $r_0 = 1.2$ nm, $a = 0.25$ nm, and $b = 2.75$ nm. While other distributions are possible, the limited signal-to-noise ratio of the present data does not allow a more detailed simulation to be performed. The suggested distribution is relatively wide, resulting in fast decay of the out-of-phase ESE with increasing τ. The absence of the pronounced oscillation pattern in the τ dependence of the out-of-phase ESE is in sharp contrast with the case of SCRPs in bacterial RCs and plant photosystems, which are characterized by a fixed interspin distance coinciding with the distance between the cofactors. This seems not to be the case for the P3HT/PCBM composite, in which the CT state is characterized by a wide distribution of the distance between the charges rather than by a fixed distance. Obviously, this is caused by the intrinsic disorder of the composite. The fixed CT state geometry used in the work of Kobori et al.[8] for the simulation of TR EPR spectra of the CT state in a P3HT/PCBM composite would lead to pronounced oscillations of the out-of-phase ESE, which are not observed. The deviation of the dipolar interaction tensor from axial symmetry assumed in the present work also contributes to fast out-of-phase echo decay. $G(r)$ most probably also depends on T_{DAF}, with larger distances prevailing at longer T_{DAF} values. Furthermore, $G(r)$ probably changes with temperature. We plan to address these issues in future work.

The out-of-phase ESE decays quite rapidly with increasing T_{DAF}. The monoexponential fit results in a characteristic decay time of 550 ns (Figure S6 in the Supporting Information). In principle, such fast decay can be caused by a very short T_1 value for $P3HT^+$ and/or $PCBM^-$. However, such short relaxation times are unlikely. A more realistic origin of this decay is polaron migration on the submicrosecond time scale, which would lead to dissociation of the CT state and loss of the magnetic interaction between its components. Also, recombination of some fraction of the CT states could contribute to the observed ESE decay rate. The obtained value of the out-of-phase ESE decay lifetime is close to the low-temperature limit of the CT lifetime in a P3HT/PCBM composite measured by transient optical absorption.[13] This limit is reached below 50 K and equals several microseconds.

The characteristic time of the in-phase ESE recovery with increasing T_{DAF} is appreciably longer, on the order of 10 μs (Figure S7 in the Supporting Information). This can be explained by recombination of the $P3HT^+/PCBM^-$ radical pairs that are stabilized at the longer distances and do not exhibit spin correlation. The components of such pairs acquire net polarizations of the same magnitude and opposite sign as a result of the chemically induced dynamic electron polarization effect.[38] However, as can be seen in Figures S3 and S4 in the Supporting Information, net emissive polarization dominates in the flash-induced ED EPR spectra. While the identification of the origin of the in-phase ESE signal at short T_{DAF} is beyond the scope of this paper, one possible mechanism can be suggested. Such a signal may originate from thermalized polarons in the vicinity of the P3HT−PCBM interface that become polarized in the course of charge separation and fast geminate recombination of $P3HT^+$ and $PCBM^-$. Such an effect was observed in a prereduced bacterial RC, in which a nonequilibrium three-spin system is formed upon laser excitation.[39] Recently, polarization of the "observer" spin of the stable radical by the SCRP was detected for a three-spin donor−acceptor−observer system.[32] Similar to our case, the emissive polarization of the stable radical prevailed. The possibility of this effect was also shown theoretically.[40,41]

The in-phase ESE recovery time with increasing delay after the laser flash defines the lower limit of T_1 for the $P3HT^+$ and $PCBM^-$ spins in the CT state. Very similar ESE recovery times were obtained for $P3HT^+$ (Figure S7 in the Supporting Information) and $PCBM^-$ (data not shown). Thus, the spin−lattice relaxation times for these spins are not shorter than 10 μs. This is an order of magnitude longer than the T_1 values determined for $P3HT^+$ and $PCBM^-$ from TR EPR[8] and CW EPR[42] (in both studies, T_1 values close to 1 μs were reported for $P3HT^+$ and $PCBM^-$). This discrepancy can be caused by the complicated procedure for simulation of the TR EPR and CW EPR spectra of the $P3HT^+/PCBM^-$ state. On the contrary, in the present work T_1 was estimated directly from the ESE recovery.

An even stronger discrepancy is noted between the T_2 values for $P3HT^+$ and $PCBM^-$ measured in the present work (about 1 μs for both species) and those obtained previously from TR EPR[8] (about 10 ns) and CW EPR[42] (in the range 20−100 ns) at close temperatures. This can be explained by the appreciable inhomogeneous broadening of the EPR spectra of $P3HT^+$ and $PCBM^-$ caused by unresolved hyperfine interactions and **g**-tensor anisotropy. This broadening severely complicates the determination of spin relaxation times from EPR spectra but does not affect the rate of ESE decay, from which T_2 is determined directly.

Finally, we should note that the proposed geometrical model of the CT state (Figure 4) is not unique, and we were able to achieve out-of-phase ESE fits of similar quality with other spin density distributions (data not shown). Also, it is possible that the exchange interaction contributes noticeably to the ESE modulation frequency.[22,31] Therefore, Figure 4 is a highly simplified schematic model of the CT state at the P3HT−

DOI: 10.1021/acs.jpcb.5b02142
J. Phys. Chem. B 2015, 119, 13543−13548

PCBM interface. For a reliable determination of the structure of this state, more detailed data are needed. Such data can be obtained in a multifrequency ESE study, which is in progress.

CONCLUSIONS

Registration of the two-pulse out-of-phase ESE from the light-induced interfacial CT state in a P3HT/PCBM composite confirms the spin-correlated nature of this state. The characteristic time of the out-of-phase ESE decay with increasing T_{DAF} is 0.5 μs at 65 K, which gives an estimation of the lifetime of these states. The dependence of the out-of-phase ESE on τ is characterized by quick decay and the absence of a pronounced oscillation pattern. From this dependence it has been derived that the CT state in the P3HT/PCBM composite should be described by a broad distribution of the interspin distances rather than by a fixed distance. The average distance between $P3HT^+$ and $PCBM^-$ in the CT state is 2−3 nm. For correct simulation of the decay of the out-of-phase ESE, the delocalization of the hole on the P3HT chain should be taken into account.

ASSOCIATED CONTENT

Supporting Information

Molecular structures of the studied substances, light-induced CW EPR signal, ED spectrum with long microwave pulses, flash-induced EPR spectrum measured with short microwave pulses, in-phase T_2 measurement, and in-phase and out-of-phase signal dependences on the delay between the laser flash and the microwave pulse sequence. This material is available free of charge via the Internet at http://pubs.acs.org.

AUTHOR INFORMATION

Corresponding Author

*E-mail: chemphy@kinetics.nsc.ru. Telephone: 7-383-3332297.

Notes

The authors declare no competing financial interest.

ACKNOWLEDGMENTS

This work was supported by the Russian Foundation for Fundamental Research (Grant 15-03-07682a), by the Ministry of Science and Education of the Russian Federation, and by a Scholarship of the President of the Russian Federation (SP-3596.2013.1). The authors thank Dr. E. Reijerse (Max Planck Institute for Chemical Energy Conversion, Muelheim-an-der-Ruhr, Germany) for critical discussion of the manuscript.

REFERENCES

(1) Deibel, C.; Dyakonov, V. Polymer−Fullerene Bulk Heterojunction Solar Cells. *Rep. Prog. Phys.* **2010**, *73*, No. 096401.

(2) Mazzio, K. A.; Luscombe, C. K. The Future of Organic Photovoltaics. *Chem. Soc. Rev.* **2015**, *44*, 78−90.

(3) Dennler, G.; Forberich, K.; Scharber, M. C.; Brabec, C. J.; Tomis, I.; Hingerl, K.; Fromherz, T. Angle Dependence of External and Internal Quantum Efficiencies in Bulk-Heterojunction Organic Solar Cells. *J. Appl. Phys.* **2007**, *102*, No. 054516.

(4) Jo, J.; Na, S.-I.; Kim, S.-S.; Lee, T.-W.; Chung, Y.; Kang, S.-J.; Vak, D.; Kim, D.-Y. Three-Dimensional Bulk Heterojunction Morphology for Achieving High Internal Quantum Efficiency in Polymer Solar Cells. *Adv. Funct. Mater.* **2009**, *19*, 2398−2406.

(5) Baranovskii, S. D.; Wiemer, M.; Nenashev, A. V.; Jansson, F.; Gebhard, F. Calculating the Efficiency of Exciton Dissociation at the Interface between a Conjugated Polymer and an Electron Acceptor. *J. Phys. Chem. Lett.* **2012**, *3*, 1214−1221.

(6) Gao, F.; Inganas, O. Charge Generation in Polymer−Fullerene Bulk-Heterojunction Solar Cells. *Phys. Chem. Chem. Phys.* **2014**, *16*, 20291−20304.

(7) Few, S.; Frost, J. M.; Nelson, J. Models of Charge Pair Generation in Organic Solar Cells. *Phys. Chem. Chem. Phys.* **2015**, *17*, 2311−2325.

(8) Kobori, Y.; Noji, R.; Tsuganezawa, S. Initial Molecular Photocurrent: Nanostructure and Motion of Weakly Bound Charge-Separated State in Organic Photovoltaic Interface. *J. Phys. Chem. C* **2013**, *117*, 1589−1599.

(9) Behrends, J.; Sperlich, A.; Schnegg, A.; Biskup, T.; Teutloff, C.; Lips, K.; Dyakonov, V.; Bittl, R. Direct Detection of Photoinduced Charge Transfer Complexes in Polymer Fullerene Blends. *Phys. Rev. B* **2012**, *85*, No. 125206.

(10) Kraffert, F.; Steyrleuthner, R.; Albrecht, S.; Neher, D.; Scharber, M. C.; Bittl, R.; Behrends, J. Charge Separation in PCPDTBT:PCBM Blends from an EPR Perspective. *J. Phys. Chem. C* **2014**, *118*, 28482−28493.

(11) Deibel, C.; Strobel, T.; Dyakonov, V. Role of the Charge Transfer State in Organic Donor−Acceptor Solar Cells. *Adv. Mater.* **2010**, *22*, 4097−4111.

(12) Gelinas, S.; Rao, A.; Kumar, A.; Smith, S. L.; Chin, A. W.; Clark, J.; van der Poll, T. S.; Bazan, G. C.; Friend, R. H. Ultrafast Long-Range Charge Separation in Organic Semiconductor Photovoltaic Diodes. *Science* **2014**, *343*, 512−516.

(13) Barker, A. J.; Chen, K.; Hodgkiss, J. M. Distance Distributions of Photogenerated Charge Pairs in Organic Photovoltaic Cells. *J. Am. Chem. Soc.* **2014**, *136*, 12018−12026.

(14) Franco, L.; Toffoletti, A.; Ruzzi, M.; Montanari, L.; Carati, C.; Bonoldi, L.; Po, R. Time-Resolved EPR of Photoinduced Excited States in a Semiconducting Polymer/PCBM Blend. *J. Phys. Chem. C* **2013**, *117*, 1554−1560.

(15) Niklas, J.; Beaupre, S.; Leclerc, M.; Xu, T.; Yu, L.; Sperlich, A.; Dyakonov, V.; Poluektov, O. G. Photoinduced Dynamics of Charge Separation: From Photosynthesis to Polymer−Fullerene Bulk Heterojunctions. *J. Phys. Chem. B* **2015**, DOI: 10.1021/jp511021v.

(16) Pasimeni, L.; Franco, L.; Ruzzi, M.; Mucci, A.; Schenetti, L.; Luo, C.; Guldi, D. M.; Kordatos, K.; Prato, M. Evidence of High Charge Mobility in Photoirradiated Polythiophene−Fullerene Composites. *J. Mater. Chem.* **2001**, *11*, 981−983.

(17) Pasimeni, L.; Ruzzi, M.; Prato, M.; Da Ros, T.; Barbarella, G.; Zambianchi, M. Spin Correlated Radical Ion Pairs Generated by Photoinduced Electron Transfer in Composites of Sexithiophene/Fullerene Derivatives: A Transient EPR Study. *Chem. Phys.* **2001**, *263*, 83−94.

(18) Uvarov, M. N.; Kulik, L. V. Electron Spin Echo of Photoinduced Spin-Correlated Polaron Pairs in P3HT:PCBM Composite. *Appl. Magn. Reson.* **2013**, *44*, 97−106.

(19) Uvarov, M. N.; Popov, A. G.; Lukina, E. A.; Kulik, L. V. Spin Relaxation and Structure of Light-Induced Spin-Correlated $PCBM^-$/$P3HT^+$ Radical Pairs. *J. Struct. Chem.* **2014**, *4*, 644−650.

(20) Bittl, R.; Zech, S. G. Pulsed EPR Spectroscopy on Short-Lived Intermediates in Photosystem I. *Biochim. Biophys. Acta* **2001**, *1507*, 194−211.

(21) Lubitz, W.; Lendzian, F.; Bittl, R. Radicals, Radical Pairs and Triplet States in Photosynthesis. *Acc. Chem. Res.* **2002**, *35*, 313−320.

(22) Dzuba, S. A.; Gast, P.; Hoff, A. J. Probing the Energy Landscape of Bacterial Photosynthetic Reaction Centers at Cryogenic Temperatures by ESEEM of Spin-Polarised $D^+Q_A^-$ Radical Pairs. *Chem. Phys. Lett.* **1997**, *268*, 273−279.

(23) Bittl, R.; Zech, S. G. Pulsed EPR Study of Spin-Coupled Radical Pairs in Photosynthetic Reaction Centers: Measurement of the Distance between $P_{700}^{\bullet+}$ and $A_1^{\bullet-}$ in Photosystem I and between $P_{865}^{\bullet+}$ and $Q_A^{\bullet-}$ in Bacterial Reaction Centers. *J. Phys. Chem. B* **1997**, *101*, 1429−1436.

(24) Fursman, C. E.; Hore, P. J. Distance Determination in Spin-Correlated Radical Pairs in Photosynthetic Reaction Centres by Electron Spin Echo Envelope Modulation. *Chem. Phys. Lett.* **1999**, *303*, 593−600.

DOI: 10.1021/acs.jpcb.5b02142
J. Phys. Chem. B 2015, 119, 13543−13548

(25) Borovykh, I. V.; Gast, P.; Dzuba, S. A. "Glass Transition" near 200 K in the Bacterial Photosynthetic Reaction Center Protein Detected by Studying the Distances in the Transient $P^+Q_A^-$ Radical Pair. *J. Phys. Chem. B* **2005**, *109*, 7535−7539.
(26) Hara, H.; Dzuba, S. A.; Kawamori, A.; Akabori, K.; Tomo, T.; Satoh, K.; Iwaki, M.; Itoh, S. The distance between P_{680} and Q_A in Photosystem II determined by ESEEM Spectroscopy. *Biochim. Biophys. Acta* **1997**, *1322*, 77−85.
(27) Dzuba, S. A.; Hara, H.; Kawamori, A.; Iwaki, M.; Itoh, S.; Tsvetkov, Y. D. Electron Spin Echo of Spin-Polarised Radical Pairs in Intact and Quinone-Reconstituted Plant Photosystem I Reaction Centres. *Chem. Phys. Lett.* **1997**, *264*, 238−244.
(28) Zech, S. G.; van der Est, A. J.; Bittl, R. Measurement of Cofactor Distances Between $P_{700}^{\bullet+}$ and $A_1^{\bullet-}$ in Native and Quinone-Substituted Photosystem I Using Pulsed Electron Paramagnetic Resonance Spectroscopy. *Biochemistry* **1997**, *36*, 9774−9779.
(29) Bittl, R.; Zech, S. G.; Fromme, P.; Witt, H. T.; Lubitz, W. Pulsed EPR Structure Analysis of Photosystem I Single Crystals: Localization of the Phylloquinone Acceptor. *Biochemistry* **1997**, *36*, 12001−12004.
(30) Savitsky, A.; Dubinskii, A. A.; Flores, M.; Lubitz, W.; Mobius, K. Orientation-Resolving Pulsed Electron Dipolar High-Field EPR Spectroscopy on Disordered Solids: I. Structure of Spin-Correlated Radical Pairs in Bacterial Photosynthetic Reaction Centers. *J. Phys. Chem. B* **2007**, *111*, 6245−6262.
(31) Carmieli, R.; Mi, Q.; Ricks, A. B.; Giacobbe, E. M.; Mickley, S. M.; Wasielewski, M. R. Direct Measurement of Photoinduced Charge Separation Distances in Donor−Acceptor Systems for Artificial Photosynthesis Using OOP-ESEEM. *J. Am. Chem. Soc.* **2009**, *131*, 8372−8373.
(32) Colvin, M. T.; Carmieli, R.; Miura, T.; Richert, S.; Gardner, D. M.; Smeigh, A. L.; Dyar, S. M.; Conron, S. M.; Ratner, M. A.; Wasielewski, M. R. Electron Spin Polarization Transfer from Photogenerated Spin-Correlated Radical Pairs to a Stable Radical Observer Spin. *J. Phys. Chem. A* **2013**, *117*, 5314−5325.
(33) Tang, J.; Thurnauer, M. C.; Kubo, A.; Hara, H.; Kawamori, A. Anomalous Pulse-Angle and Phase Dependence of Hahn's Electron Spin Echo and Multiple-Quantum Echoes in a Photoinduced Spin-Correlated Radical Pair. *J. Chem. Phys.* **1997**, *106*, 7471−7478.
(34) Hoff, A. J.; Gast, P.; Dzuba, S. A.; Timmel, C. R.; Fursman, C. E.; Hore, P. J. The Nuts and Bolts of Distance Determination and Zero- and Double-Quantum Coherence in Photoinduced Radical Pairs. *Spectrochim. Acta, Part A* **1998**, *54*, 2283−2293.
(35) Moenne-Loccoz, P.; Heathcote, P.; Maclachlan, D. J.; Berry, M. C.; Davis, I. H.; Evans, M. C. W. Path of Electron Transfer in Photosystem 1: Direct Evidence of Forward Electron Transfer from A_1 to Fe−S_X. *Biochemistry* **1994**, *33*, 10037−10042.
(36) Holdcroft, S. A Photochemical Study of Poly(3-hexylthiophene). *Macromolecules* **1991**, *24*, 4834−4838.
(37) Niklas, J.; Mardis, K. L.; Banks, B. P.; Grooms, G. M.; Sperlich, A.; Dyakonov, V.; Beaupre, S.; Leclerc, M.; Xu, T.; Yu, L.; Poluektov, O. G. Highly-Efficient Charge Separation and Polaron Delocalization in Polymer −Fullerene Bulk-Heterojunctions: A Comparative Multi-Frequency EPR and DFT Study. *Phys. Chem. Chem. Phys.* **2013**, *15*, 9562−9574.
(38) Hore, P. J. Transfer of Spin Correlation between Radical Pairs in the Initial Steps of Photosynthetic Energy Conversion. *Mol. Phys.* **1996**, *89*, 1195−1202.
(39) Borovykh, I. V.; Kulik, L. V.; Dzuba, S. A.; Hoff, A. J. Out-of-Phase Stimulated ESE Appearing in the Evolution of Spin-Correlated Photosynthetic Triplet-Radical Pairs. *J. Phys. Chem. B* **2002**, *106*, 12066−12071.
(40) Salikhov, K. M.; van der Est, A. J.; Stehlik, D. The Transient EPR Spectra and Spin Dynamics of Coupled Three-Spin Systems in Photosynthetic Reaction Centres. *Appl. Magn. Reson.* **1999**, *16*, 101−134.
(41) Salikhov, K. M.; Zech, S. G.; Stehlik, D. Light Induced Radical Pair Intermediates in Photosynthetic Reaction Centres in Contact with an Observer Spin Label: Spin Dynamics and Effects on Transient EPR Spectra. *Mol. Phys.* **2002**, *100*, 1311−1321.
(42) Krinichnyi, V. I.; Yudanova, E. I.; Spitsina, N. G. Light-Induced Electron Paramagnetic Resonance Study of Poly(3-alkylthiophene)/Fullerene Composites. *J. Phys. Chem. C* **2010**, *114*, 16756−16766.

DOI: 10.1021/acs.jpcb.5b02142
J. Phys. Chem. B 2015, 119, 13543−13548